FATIGUE CRACK FORMATION AND PROPAGATION IN PAVEMENTS CONTAINING SOIL-CEMENT BASES

P. C. Pretorius, Bruinette, Kruger, Stoffberg and Hugo, Johannesburg, South Africa; and
C. L. Monismith, Institute of Transportation and Traffic Engineering, University of California, Berkeley

In this report an attempt is made to predict the formation and development of fatigue cracks in pavements containing soil-cement bases. It is assumed that transverse shrinkage cracks have already formed. To obtain realistic results, we analyzed a typical pavement section consisting of 3 in. of asphalt concrete and 8 in. of cement-treated base resting on a clayey subgrade. The properties of the cement-treated base were developed from an extensive laboratory investigation, and the fatigue results obtained are reported in some detail. These results confirm previous fatigue studies performed by the Portland Cement Association. To estimate the stresses in a pavement system with transverse shrinkage cracks present and thus to estimate the potential for fatigue cracking, we used a prismatic-space finite-element procedure. The results of the analysis show that the first fatigue crack to develop is perpendicular to the shrinkage crack and in the position of the wheelpath. A crack of this type may propagate fairly rapidly because of stress concentrations at the tip of the crack and lead to the "corner loading" situation bounded by the shrinkage and perpendicular fatigue cracks. This situation can be analyzed approximately by using the Westergaard formula, i.e., transforming the asphalt concrete layer to an equivalent thickness of cement-treated base. The stresses resulting from this analysis indicate the potential for additional load-associated cracking leading to the possibility for the corner to break off. Because this situation can repeat itself with continued load repetitions, the familiar double-ladder crack pattern is established. It is also shown that the presence of a longitudinal shrinkage crack parallel and close to the fatigue crack may give rise to a single-ladder crack pattern. The crack pattern predictions are substantiated to some degree by a field investigation. The propagation of load-associated cracks was traced by periodically photographing an underdesigned pavement containing a cement-treated base over a period of time during which rapid deterioration due to repeated loading occurred.

•IN a previous paper (1) it was shown how the formation and spacing of shrinkage cracks in pavements containing soil-cement bases could be predicted by using laboratory measured material characteristics together with an incremental finite-element solution for a system representative of the pavement structure. Material characteristics included measured values for shrinkage, creep, and strength (both tensile and compressive). Although such an approach may be of interest to the researcher, it may hold less significance for the practicing engineer because the formation of shrinkage cracks in soil cement is generally inevitable (2). Of more significance are the consequences of shrinkage cracking because such cracking may contribute to a rapid deterioration in pavement serviceability under certain circumstances.

Sponsored by Committee on Theory of Pavement Design.

The primary purpose of this paper is to illustrate how load cracks can propagate from a shrinkage crack and includes a discussion of some of the variables that influence the crack pattern and rate of crack propagation. Observations of the performance of an in-service pavement during a 5-month period are included to show the validity of this procedure.

METHOD

The approach used in this investigation involved the selection for analysis of a pavement containing a soil-cement base consisting of 3 in. of asphalt concrete and 8 in. of soil cement resting on a clayey subgrade.

Stiffness characteristics of the asphalt concrete and clayey subgrade were selected on the basis of experience with such materials in previous investigations, recognizing temperature and time of loading effects for the asphalt concrete and stress effects for the subgrade material. Data for the soil cement were the same as reported earlier (1). This material consisted of a partially crushed gravel (gradation shown in Fig. 1) treated with 5.5 percent by weight of cement, which satisfied the wet-dry test of the Portland Cement Association.

Because this aspect of the study was concerned with load-associated cracking of the soil cement, an extensive fatigue investigation was conducted on the cement-treated material, results of which will be detailed in a subsequent section.

To analyze the load-associated stresses in the vicinity of a transverse shrinkage crack, we used the prismatic space finite-element method (3). This analysis procedure is essentially two-dimensional with the third dimension introduced into the idealization by expressing the load as Fourier Series in the third direction. A finite-element discreteness of the structure is shown in Figure 2. A particular structure is solved for every Fourier term necessary to adequately represent the load. The x and y displacements vary cosinusoidally and the stresses sinusoidally in the z direction, which allows a complete stress and strain solution at any desired z position. Unfortunately, the program is time-consuming because a complete finite-element solution is required for every Fourier term required to represent the load. Usually, 10 to 15 such terms produce satisfactory results.

Maximum stresses corresponding to the post-cracked situation can then be compared to the stresses obtained for the internal (uncracked) loading condition (by using either the axisymmetric finite-element approach or the Chevron 5-layer computer program). By comparing fatigue lives corresponding to each loading condition, we can establish the first fatigue crack, and, depending on other influences, a prediction of the pattern of crack propagation may be possible.

FATIGUE INVESTIGATION

Comparatively few data have been reported for soil cement subjected to fatigue loading. Bofinger (4) in a follow-up to an earlier investigation reported for cement-treated soil that a higher cement content increases fatigue life, presoaking drastically reduces fatigue life, and an increase in initial dry density increases fatigue life.

Bofinger prefers direct tension to flexural fatigue testing because the elastic modulus of soil cement in tension differs from that in compression. It should be realized, however, that the fatigue life is sensitive to stress and strain gradients, and results of direct tension fatigue tests (zero stress gradient) can be considered as a lower bound for the fatigue life. In the opinion of the authors, flexural testing is a better simulation of actual field behavior because a stress gradient always exists in cement-treated base subjected to load. By measuring tensile and compressive strains in a laboratory test specimen, we can account for bi-modulus effects. There is also evidence that the standard briquettes (used by Bofinger) are subject to stress concentrations with the result that the stress that actually causes fatigue deterioration is unknown.

The most comprehensive fatigue investigation on soil cement reported to date is that by Larsen and Nussbaum (5). From tests on 3 soil types with 4 beam depths and

4 simulated subgrade moduli as variables, a relation was established as follows:

$$R_c/R = a\,N^{-b}$$

where

R_c = radius of curvature at failure (critical radius of curvatuve),
R = radius of curvature developed for a given load and number of load applications,
a and b = coefficients, and
N = number of load repetitions.

Their test results indicated that the coefficient b, i.e., slope of the line on a semi-logarithmic plot, is dependent only on soil type; subgrade strength had no influence; and the coefficient a decreased with increasing specimen thickness and is independent of soil type.

Some of their measurements may have been influenced by the ratio of span length to beam depth (deep beam action). For small span length-to-depth ratios, the stress and strain distributions are no longer linear, which makes it difficult to compare fatigue results.

Figure 3 shows what can be expected under "deep beam action" and also illustrates the influence of a compression-to-tension modulus ratio that is greater than unity. These results were obtained by means of a plane stress finite-element analysis.

Specimens and Procedures

Specimens for fatigue testing consisted of beams 3 in. by 3 in. in cross section and 18 in. long, prepared by vibratory compaction in three layers perpendicular to the longitudinal axis. After curing overnight in a 100 percent relative humidity environment, the specimens were removed from their molds and the densities were determined; the specimens were then wrapped in polyethelene sheets and returned to the 100 percent relative humidity environment for a curing period of at least 3 months. (A minimum period of 3 months was selected in order to minimize curing effects during testing.)

Average properties for the specimens tested were as follows:

1. Stiffness modulus—2.8×10^6 psi;
2. Compressive strength, 28 days—1,000 psi;
3. Flexural strength (modulus of rupture), 28 days—200 psi; and
4. Direct tensile strength, 28 days—100 psi.

Fatigue tests were conducted in a closed-loop vibration testing system. Repeated loading was applied by using the haversine input function, which is defined by

$$P(\theta) = \tfrac{1}{2}(1 - \cos\theta)$$

Of the available load forms in this type of equipment, the haversine function appears to best represent actual field loading conditions.

Third-point loading at a frequency of 2 cps was utilized for the fatigue tests, and all specimens subjected to fatigue loading were conditioned at a total load of 250 lb (approximately 38 percent of ultimate flexural strength) for at least 500 cycles prior to fatigue testing. Strains were measured by bonded-wire gauges with a gauge length of 2.5 in. cemented to both the top and bottom surfaces of each beam.

Some preliminary studies were conducted to investigate rate of loading effects on material stiffness, which in turn might provide an indirect indication of rate effects on fatigue life. Results of these studies, briefly summarized in Appendix A, indicate that the stiffness characteristics are sensibly independent of rate of loading effects in the frequency range of 0.01 to 10 cps.

Results

A total of 31 specimens was tested in flexural fatigue. Fatigue life as a function of initial maximum flexural strain in tension is shown in Figure 4. As might be expected,

Figure 1. Gradation curve, aggregate for soil cement.

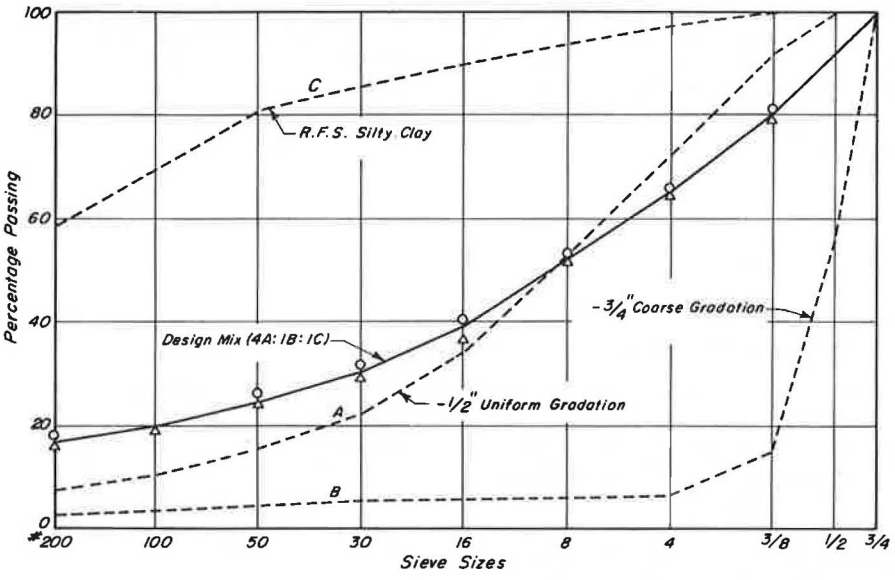

Figure 2. Prismatic-space finite-element representation.

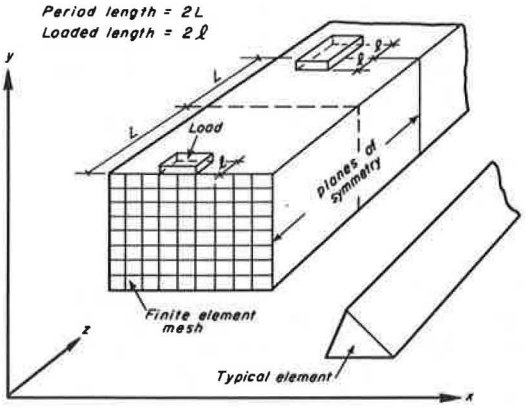

Figure 3. Stress and strain distributions in shallow and deep beams loaded at the one-third points.

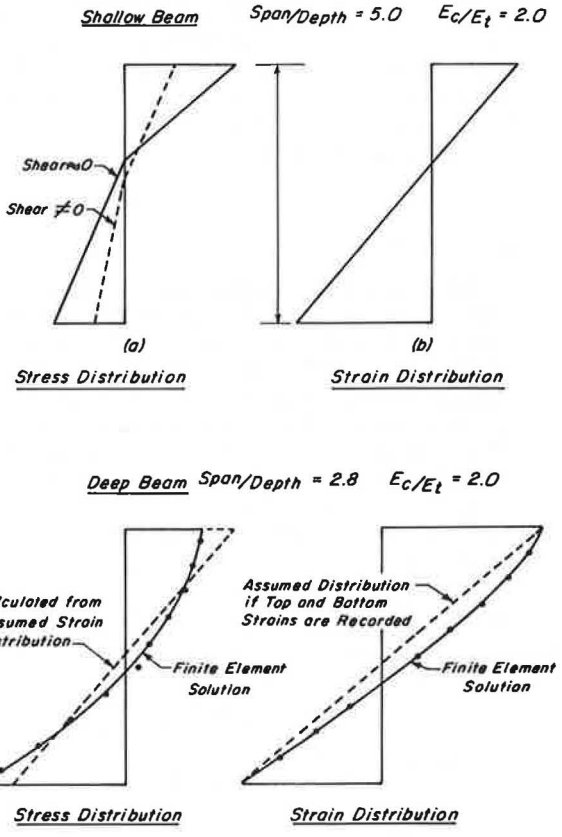

scatter is observed in the test results. Straight-line approximations to this data on semilogarithmic and full-logarithmic plots (using least squares) resulted in the equations shown in Figure 4. The slope of the fatigue curve is quite flat, which indicates considerable sensitivity of fatigue life to small strain variations and may be due, at least in part, to the high flexural stiffness of this material.

Results of this investigation could be compared with those developed by Larsen and Nussbaum (5) because radii of curvature could be obtained directly from the strain measurements, i.e.,

$$R = h/(\epsilon_t + \epsilon_b)$$

where

R = radius of curvature,
h = specimen depth, and
ϵ_t and ϵ_b = top and bottom recorded strains respectively.

A critical radius of curvature, R_c, was obtained by extrapolation of the radius of curvature versus load relation. For this material, R_c was estimated to be 10,000 in.

The resulting data are shown in Figure 5. The data confirm Larsen and Nussbaum's conclusions that the coefficient a in the expression $R_c/R = a\ N^{-b}$ is sensibly independent of soil type, whereas the coefficient b appears to increase as the material becomes more granular.

It has been suggested (6) that a study of strain history in a fatigue test might be of value in assessing the accumulation of fatigue damage. Figure 6 shows some typical flexural tensile strain histories up to failure. It is seen that the strain remains fairly constant over a large portion of the fatigue life after which the rate of change of strain starts to increase. Once the strain starts changing, it does so at an increasing rate until complete rupture is achieved.

An interesting observation in this test series was that specimens that did not fail after 1 million load applications exhibited a constant strain output during the entire test. When these specimens were then failed at a higher stress, the strain history was the same as indicated in Figure 6; also the number of load applications to failure corresponded reasonably well to the fatigue curve, which suggests that the previously induced fatigue damage was comparatively insignificant.

CRACK PROPAGATION

Analytic Study

To evaluate the importance of load transfer across a transverse crack, we obtained results for an interior load condition (i.e., away from the influence of edge effects) by using the Chevron 5-layer axisymmetric computer program. An 18-kip axle load was applied (Fig. 7) to the pavement structure (layer thickness noted earlier) with the cement-treated base assumed to have a stiffness modulus of 2.8×10^6 psi. The maximum flexural stress obtained is indicated in Figure 8; this figure shows the sensitivity of the stress in the cement-treated base to moduli changes in the other layers. The modulus chosen for the asphalt concrete represents a traffic-weighted stiffness modulus (7) corresponding to environmental conditions at Morro-Bay, California (essentially a cool coastal environment).

At a flexural tensile stress of 80 psi (Fig. 8), a fatigue life in excess of 1×10^6 equivalent 18,000-lb axle load applications would be obtained as seen in Figure 9, which contains the fatigue curve of Figure 4 plotted in terms of stress.

Once a transverse crack forms, however, a different set of circumstances exists. Increased stresses may be anticipated because of the loss of continuity (or "load transfer") and the possibility that water infiltration may weaken the subgrade (8). To obtain some estimate of these conditions we analyzed the pavement by using the prismatic-space finite-element method.

This representation of the pavement is shown in Figure 10 with transverse cracks placed at 20-ft intervals. The pavement model is continuous in the z direction, and the free edges are parallel to the z-axis.

Figure 4. Initial strain versus repetitions to fracture, flexural specimens.

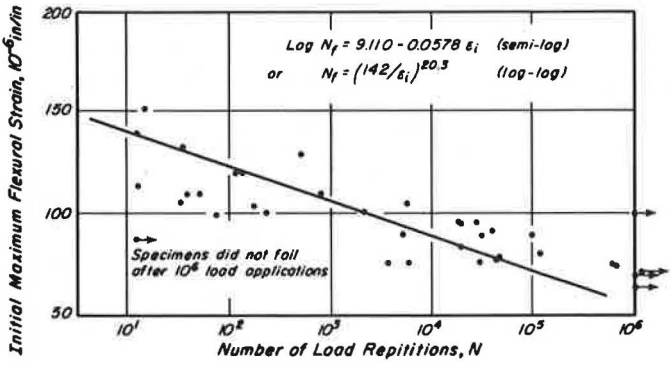

Figure 5. Comparison of fatigue results (Fig. 4) with data developed by Larsen and Nussbaum.

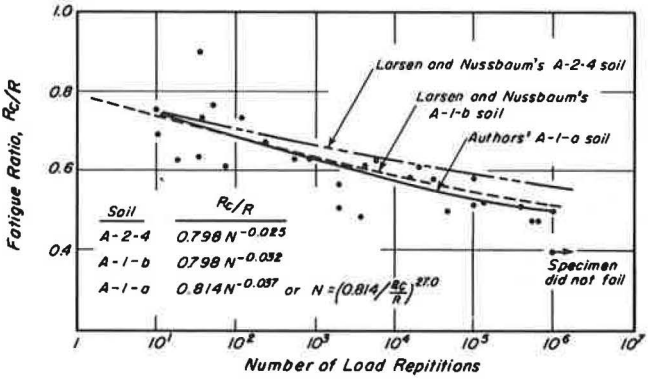

Figure 6. Strain histories of flexural fatigue specimens.

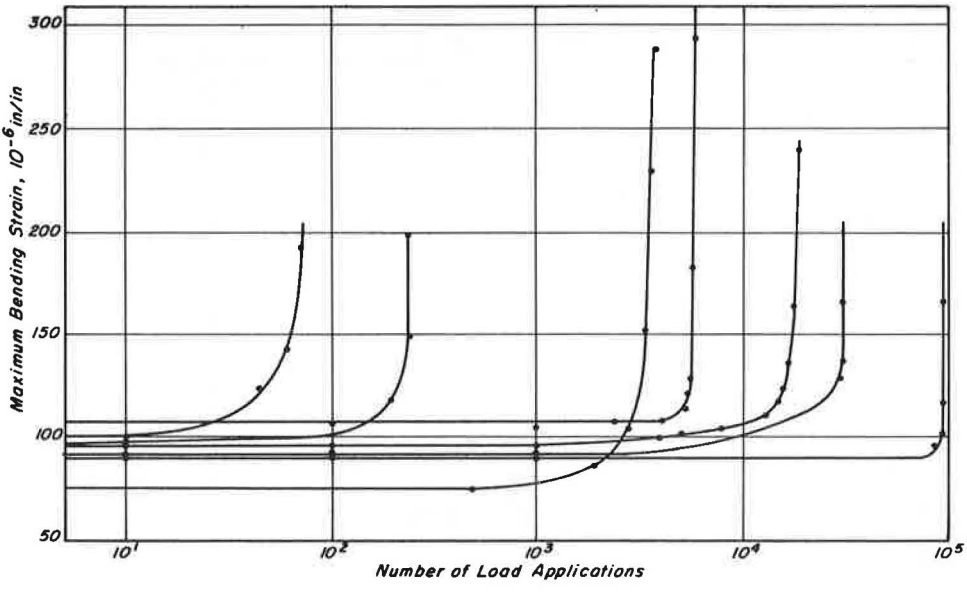

Figure 7. Assumed wheel spacing for 18,000-lb axle load.

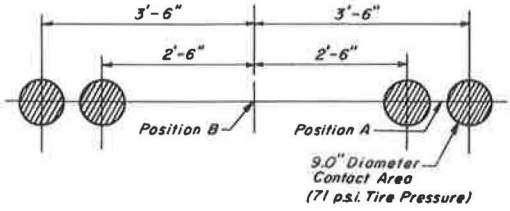

Figure 8. Maximum tensile stress on underside of soil-cement base.

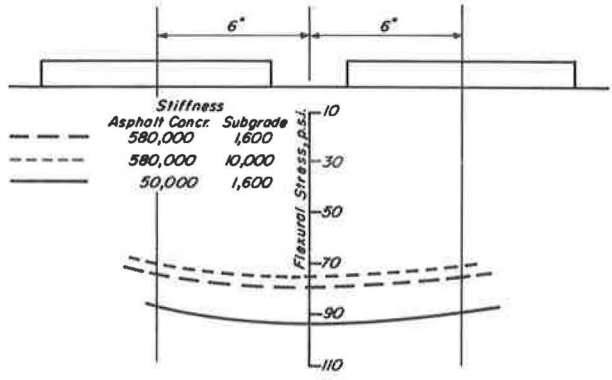

Figure 9. Stress versus repetitions to fracture, flexural specimens.

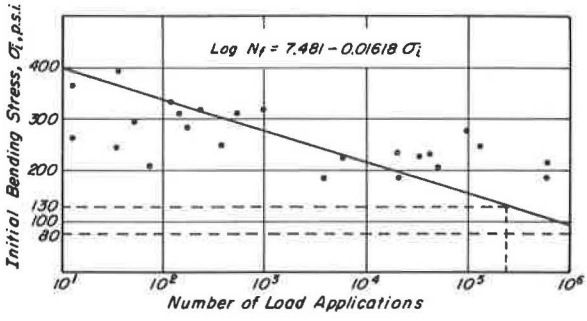

Figure 10. Finite-element mesh for load at an edge.

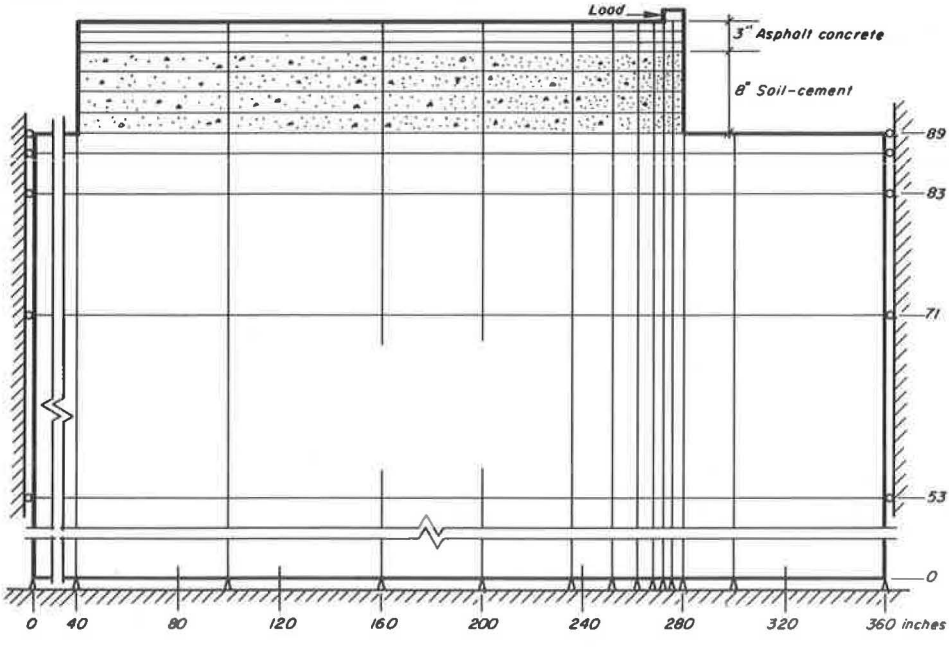

The two loading conditions shown in Figure 11, one at the cracked edge and the other slightly inward from the free edge, were analyzed. Stress contours corresponding to these loadings are shown in Figures 12 and 13. The stresses shown in these figures are not maximum stresses; rather they correspond to the stresses at the center of the upper and lower elements in the finite-element representation of the cement-treated base. The actual stress distributions are shown in Figures 14 and 15. The results indicate that maximum stress is in the z direction at position B for the loading at position BB. This stress, 130 psi, is approximately 60 percent greater than that for the corresponding axisymmetric case, and the fatigue life at this stress (Fig. 9) is considerably less. The results also indicate that fatigue in the asphalt concrete layer is not critical.

As a part of this study, four conditions of subgrade support were investigated (Fig. 21, Appexdix B). Little difference in stress was obtained (Fig. 14), although the surface deflections (Fig. 22, Appendix B) increased with a decrease in subgrade modulus. It was determined that the radius of curvature remained relatively unchanged and is in part attributable to the high modular ratio (approximately 280) of the soil cement to the subgrade, a point also noted by Whiffin and Lister (9).

These results were obtained by assuming complete loss of load transfer across the crack. For very fine cracks, a high percentage of load transfer is still possible, at least initially. However, it is possible, as noted by Colley and Humphrey (10), who measured load transfer for portland cement concrete pavements, that this transfer is reduced with number of load applications as well as with crack width.

CRACK PATTERNS

From the previous discussion, it follows that the first fatigue crack will probably be a longitudinal crack in the center of the wheelpath initiated at the bottom of the cement-treated material.

Once this crack has formed, stress concentrations at the tip of the crack will cause it to penetrate longitudinally and also to the surface. If this crack has progressed far enough, the areas bounded by the fatigue and shrinkage cracks will be subjected to corner loading conditions. Although this problem cannot be handled by the finite-element procedure at the present time, an approximate estimate of stress can be made by using the Westergaard corner loading formula. To use this relation for the asphalt concrete and cement-treated section, we converted the asphalt concrete thickness to an equivalent thickness of soil cement by using the ratio of their moduli (or stiffnesses). For these conditions, a maximum tensile stress of 111 psi was estimated to occur at a distance of about 28 in. from the corner on the diagonal (Fig. 16). As can be seen in Figure 9, this can represent a relatively severe condition for fatigue after the longitudinal crack has formed.

It should be noted that the distance along the corner diagonal is a function of the stiffness of the cement-treated base and will be shorter for more flexible layers. Moreover, load-associated cracks are also possible "normal" to the existing fatigue crack as well as "normal" to the shrinkage and parallel to the first fatigue crack (due to transverse distribution of traffic).

The potential now exists for the corner to break off as shown in Figure 16, and this process will repeat itself with continued load applications to form the familiar double-ladder crack pattern indicated.

It is possible that this crack pattern can be altered if a longitudinal shrinkage crack exists close to the longitudinal fatigue crack as is shown for the right-hand wheelpath in Figure 16. For these circumstances, a longitudinal strip exists that can be analyzed by using the finite-element procedure. For a 2-ft wide strip, for example, a maximum stress of 136 psi adjacent to and in the direction of the longitudinal crack was obtained. As noted earlier, this will lead to early cracking with the result that a single-ladder type crack pattern will now occur (Fig. 16). In all probability, these transverse fatigue cracks will be randomly spaced because the maximum stress occurs directly beneath the wheel load for this loading condition.

Figure 11. Loading positions for edge effect considerations.

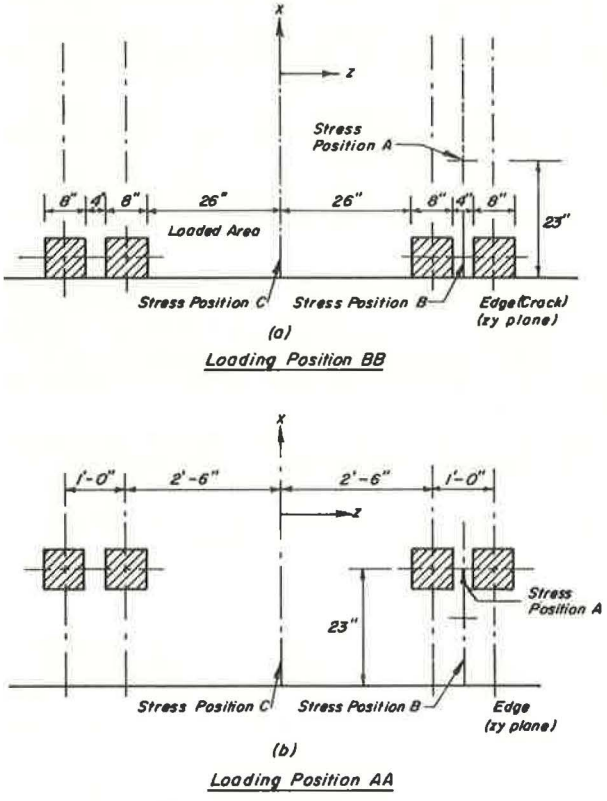

Figure 12. Stress contours for load at position BB.

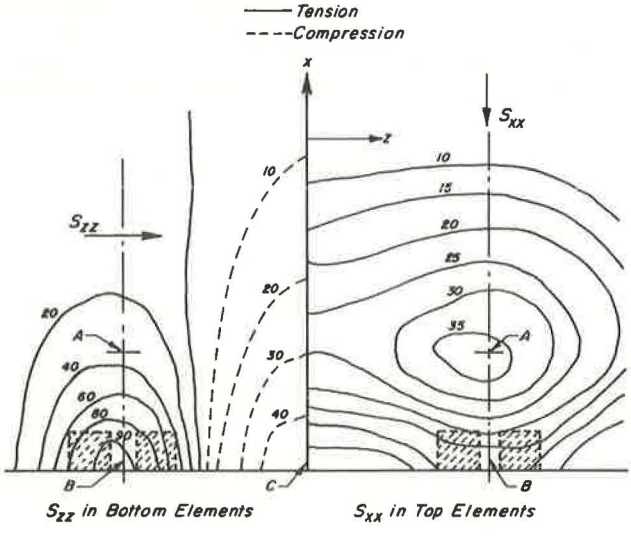

Figure 13. Stress contours for load at position AA.

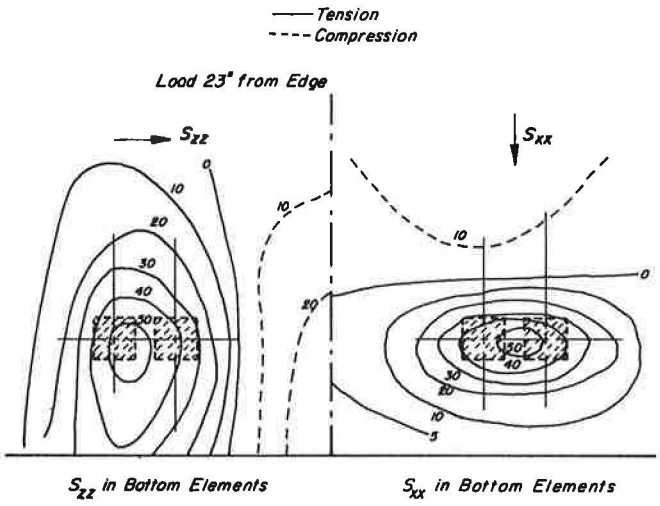

Figure 14. Distribution of stress S_{xx} at position A for loading at positions AA and BB.

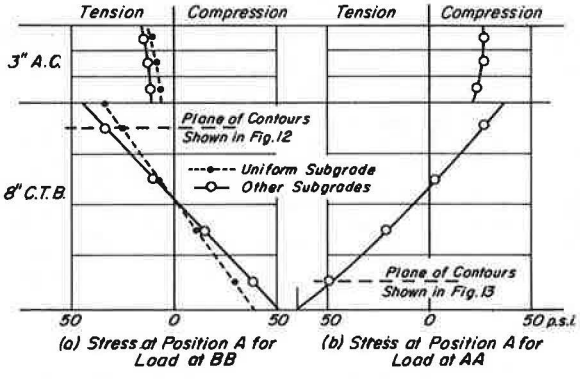

Figure 15. Distributions of stress S_{zz} with depth.

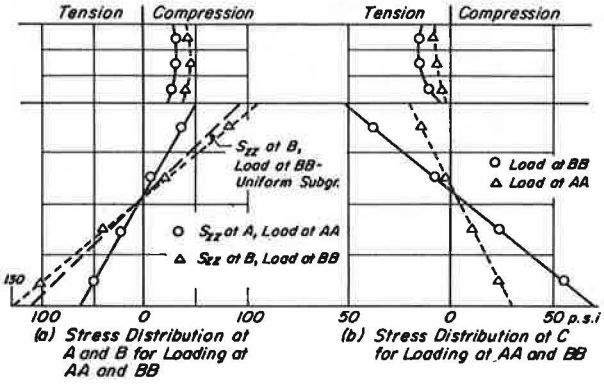

Figure 16. Crack patterns.

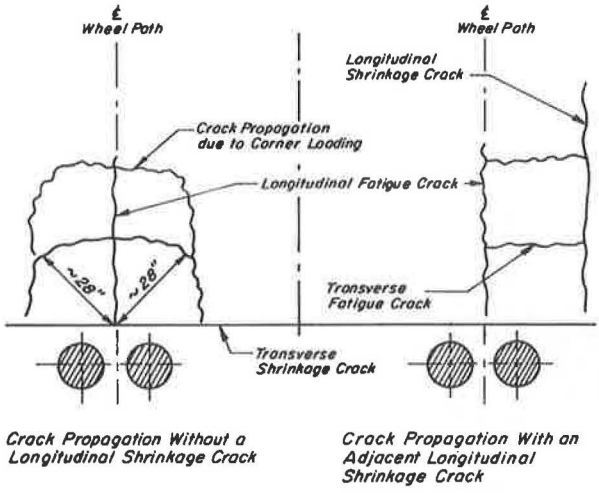

Figure 17. Crack pattern, November 11, 1970.

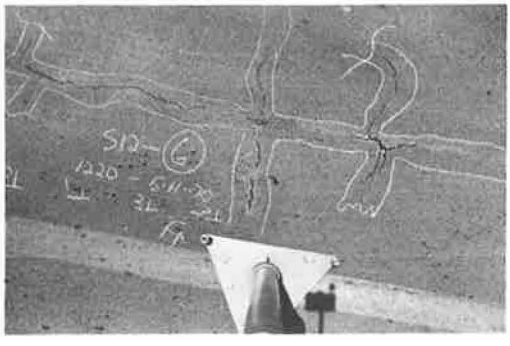

Figure 18. Crack pattern, January 20, 1971.

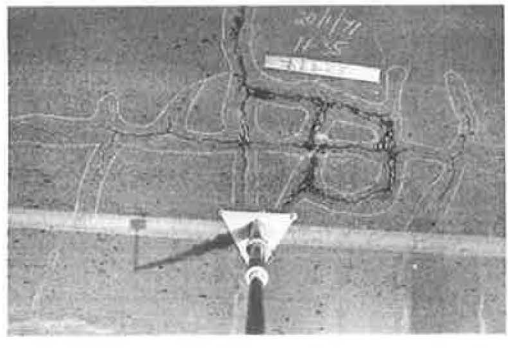

Figure 19. Crack pattern, February 22, 1971.

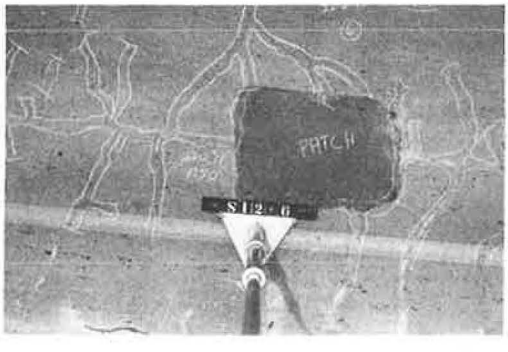

Figure 20. Overall view of pavement showing typical crack pattern.

FIELD STUDY

Subsequent to the analytic study, a recently constructed pavement near Johannesburg, South Africa, containing a soil-cement base, presented an opportunity for a field investigation of the load-associated cracking phenomenon previously described.

On this particular project, the upper 3 layers of the pavement consisted of 1 in. of asphalt concrete, 4 in. of cement-treated base, and 4 in. of compacted gravel. The cement-treated base was a crushed aggregate stabilized with 5 percent cement (by weight). The 28-day cube strength of the cement-stabilized material averaged between 1,000 and 1,500 psi.

The road serves heavy coal traffic, and roadside wheel load measurements indicated that about 10 to 20 percent of the trucks exceeded the legal axle load of 18,000 lb. Areas that showed little fatigue distress were selected, and these areas were photographed monthly by placing the camera at exactly the same position each time.

The crack propagation study, shown in Figures 17-19, covers the 4-month period from November 1970 to March 1971. January was a month of exceptionally high rainfall for the area.

The cement-treated base was laid by a paver in 10-ft wide sections, starting with the section that included the 8-ft wide shoulder. This resulted in a construction joint in the vicinity of the outer wheelpath. Consequently, longitudinal shrinkage cracks at the construction joints appeared simultaneously with transverse shrinkage cracks (spaced between 12 and 20 ft apart). Figure 17 shows these two cracks very distinctly.

This situation differs slightly from the analytic one presented previously in that the longitudinal crack is now also a shrinkage crack instead of a fatigue crack. The result is that fatigue cracks can now develop perpendicularly to either the transverse or longitudinal shrinkage cracks.

Such fatigue cracks, branching off from the longitudinal shrinkage crack, are also shown in Figure 17.

In Figure 18, taken about 10 weeks later, the double-ladder fatigue pattern is well-established. The progressive failure of a corner piece is clearly illustrated.

Figure 19 shows further deterioration after the initial failure area has been repaired.

Figure 20 shows an overall view of a typical crack pattern. It shows a number of closed fatigue cracks as well as a few in the process of closing the loop.

Studies of cracking at various locations on the same route showed the same general pattern; such results would appear to be in general agreement with the crack propagation and patterns predicted previously.

CONCLUSIONS

From the results presented herein, the following conclusions appear warranted:

1. The fatigue results tend to confirm previous research work performed by the Portland Cement Association with the exception of the case for specimens whose span lengths are short relative to their depths ("deep beams"). In this situation, the true fatigue response may differ from that predicted by the PCA results because of "deep-beam" action.
2. For the assumed situation of complete loss of load transfer across a transverse shrinkage crack in the cement-treated base, significantly larger tensile stresses may result adjacent to the crack, which in turn reduces the number of load repetitions that the section can withstand compared to its capabilities in the uncracked condition.
3. By following consecutively the locations of maximum tensile stresses as cracks develop, it is possible to predict crack patterns similar to those observed in in-service pavements as noted from the field observations reported herein.

ACKNOWLEDGMENTS

The assistance of C. K. Chan of the Institute of Transportation and Traffic Engineering in the development, design, and use of the testing equipment is gratefully acknowledged. The authors also wish to acknowledge the South African Council for Scientific and Industrial Research for the research fellowship provided to the first author.

REFERENCES

1. Pretorius, P. C., and Monismith, C. L. The Prediction of Shrinkage Stresses in Pavements Containing Soil-Cement Bases. Highway Research Record 362, 1971, pp. 63-86.
2. Wilson, E. L., and Pretorious, P. C. A Computer Program for the Analysis of Prismatic Soilds. Structural Engineering Lab., Univ. of California, Berkeley, Rept. UC SESM 70-21, 1970.
3. Pretorius, P. C. Design Consideration for Pavements Containing Soil-Cement Bases. Univ. of California, Berkeley, PhD dissertation, 1970.
4. Bofinger, H. E. Further Studies on the Tensile Fatigue of Soil-Cement. Australian Road Research, Vol. 4, No. 1, Sept. 1969.
5. Larsen, T. J., and Nussbaum, P. J. Fatigue of Soil-Cement. Jour. of Portland Cement Association Research and Development Laboratories, Vol. 9, No. 2, May 1967, pp. 37-59.
6. Raithby, K. D., and Whiffin, A. C. Failure of Plain Concrete Under Fatigue Loading—A Review of Current Knowledge. Gt. Brit. Road Research Laboratory, RRL Rept. LR231.
7. Kasianchuk, D. A. Fatigue Considerations in the Design of Asphalt Concrete Pavements. Univ. of California, Berkeley, Phd dissertation, 1968.
8. Williams, A. A. B., and Dehlen, G. L. The Performance of Full-Scale Base and Surfacing Experiments on National Route 3-1, at Key Ridge, After the First Six Years. First Conf. on Asphalt Pavements for Southern Africa, Durban, Aug. 1969.
9. Whiffin, A. C., and Lister, N. W. The Application of Elastic Theory to Flexible Pavements. Internat. Conf. on Structural Design of Asphalt Pavements, Ann Arbor, Mich., 1962.
10. Colley, B. E., and Humphrey, H. A. Aggregate Interlock at Joints in Concrete Pavements. Highway Research Record 189, 1967, pp. 1-18.
11. Papazian, H. S. The Response of Linear Visco-Elastic Materials in the Frequency Domain. Transportation Eng. Center, Eng. Exp. Station, Ohio State Univ., Columbus, Rept. 172-2, 1961.

APPENDIX A

RATE OF LOADING STUDY FOR SOIL CEMENT

In an initial part of the study, surface strains were measured both statically and dynamically on specimens of the soil cement. Linear strain distributions (for all practical purposes) were observed in both types of tests to failure.

Rate of loading effects were observed by defining a complex modulus of the material over a frequency range for loading of 0.01 to 10 cps. The phase angle, ϕ, by which the strain lagged the applied stress was extremely small, indicating essentially elastic response.

The same conclusion was reached from an analysis of the results of short-time creep experiments, which yielded the following results:

$$\text{elastic modulus } E = \frac{\text{initial stress}}{\text{initial strain}} = 2.43 \times 10^6 \text{ psi}$$

$$\text{viscous traction } \lambda = \frac{\text{stress}}{\text{rate of change of strain}} = 7.80 \times 10^9 \text{ psi/sec}$$

$$\text{retardation time } \tau = \lambda/E = 3{,}210 \text{ sec}$$

The phase angle lag can then be estimated from the following (11):

$$\phi = \tan^{-1}(E/\omega\lambda) \tan^{-1}(1/3{,}210\ \omega)$$

where ω = frequency of loading. In the frequency range of 0.01 to 10 cps, it can be seen that ϕ will be quite small, thus substantiating the observations in dynamic loading.

For the range of loading conditions studied herein, the soil cement can, for practical purposes, be considered an "elastic" material.

APPENDIX B

SUBGRADE SUPPORT CONDITIONS

Figure 21.

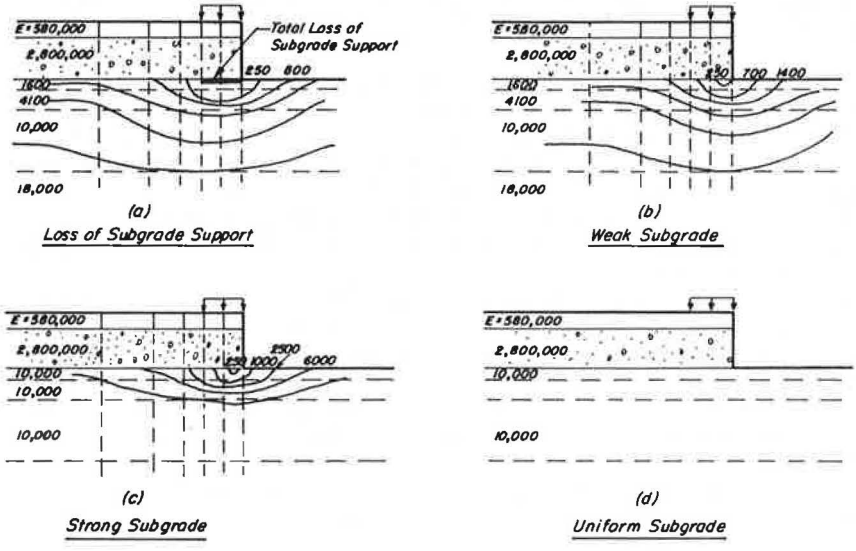

Figure 22.